

# Ground state energy of spin-1/2 fermions in the unitary limit

Dean Lee

*Department of Physics, North Carolina State University, Raleigh, NC 27695*

## Abstract

We present lattice results for the ground state energy of a spin-1/2 fermion system in the unitary limit, where the effective range of the interaction is zero and the scattering length is infinite. We compute the ground state energy for a system of 6, 10, 14, 18, and 22 particles, with equal numbers of up and down spins in a periodic cube. We estimate that in the limit of large number of particles, the ground state energy is 0.25(3) times the ground state energy of the free Fermi system.

## I. INTRODUCTION

The unitary limit of spin-1/2 or two-component fermions has attracted much recent experimental and theoretical interest from several branches of physics. The term unitary limit or unitary regime refers to the idealized limit where the effective range of the interaction is zero and the scattering length is infinite. Much of the interest has been spurred by experimental advances in the trapping of ultracold atomic Fermi gases. Starting with a dilute Fermi gas, where the effective range of the interaction is negligible compared with the interparticle spacing, one can reach the unitary limit by tuning the scattering length to infinity using a Feshbach resonance [1, 2, 3, 4, 5, 6, 7].

In nuclear physics the unitary limit is directly relevant to the properties of cold dilute neutron matter. The neutron scattering length is roughly  $-18$  fm while the effective range is  $2.8$  fm. Therefore the unitary limit is approximately realized when the interparticle spacing is about  $5 - 10$  fm, roughly  $0.5\% - 5\%$  of normal nuclear matter density, which is believed to be relevant to the physics of the inner crust of neutron stars [8].

At zero temperature in the unitary limit there are no dimensionful parameters other than the particle density. Therefore the ground state energy of the system should obey a simple relation  $E^0 = \xi E^{0,\text{free}}$ , where  $E^{0,\text{free}}$  is the ground state energy of a non-interacting Fermi gas and  $\xi$  is a dimensionless constant. Recent experiments have measured the expansion of  ${}^6\text{Li}$  in the unitary limit released from a harmonic trap [6, 7]. Based on a Thomas-Fermi model, the measured values for  $\xi$  are  $0.51(4)$  [6] and  $0.32^{+10}_{-13}$  [7]. The discrepancy between these two recent measurements and with larger values for  $\xi$  reported in earlier experiments [1, 4, 5] suggest further experimental work is needed, as well as a better theoretical understanding of Thomas-Fermi theory and other local density approximations in the unitary limit.

There have been several recent analytic calculations of  $\xi$  using various techniques such as BCS saddle point and variational approximations, Padé approximations, mean field theory with pairing, and dimensional expansions [9, 10, 11, 12, 13]. The values for  $\xi$  vary from roughly  $0.3$  to  $0.6$ . Fixed-node Green's function Monte Carlo calculations have found  $\xi$  to be  $0.44(1)$  [14] and  $0.42(1)$  [15]. A recent estimate based on Kohn-Sham theory for the two-fermion system in a harmonic trap yields a value of  $0.42$  [16]. Recently there have also been simulations of spin-1/2 fermions on the lattice in the unitary limit [17, 18, 19, 20]. While the simulations are at nonzero temperature, the results can be extrapolated to provide an

estimate for  $\xi$ . The results of [18] produced a value for  $\xi$  similar to the fixed-node results, while [20] established a bound,  $0.07 \leq \xi \leq 0.42$ .

In this paper we describe a new calculation of  $\xi$  on the lattice at zero temperature and fixed particle number. In contrast with Green's function Monte Carlo, the method we describe is free from the fermion sign problem. Because of this we can eliminate systematic errors due to fermion nodal constraints. Using a new algorithm which combines endpoint correlation function importance sampling and non-local Monte Carlo updating, we measure the ground state energy for 6, 10, 14, 18, and 22 particles, with equal numbers of up and down spins in a periodic cube. We estimate that in the limit of large number of particles, the ground state energy is 0.25(3) times the ground state energy of the free Fermi system.

## II. LATTICE FORMALISM

We refer to the state with  $N$  spin-up fermions and  $N$  spin-down fermions as an  $N, N$  state. We use the same lattice action as described in [19, 20, 21]. Since we will be working at fixed particle number we can set the chemical potential to zero. Throughout we use dimensionless parameters and operators, which correspond with physical values multiplied by the appropriate power of the spatial lattice spacing  $a$ . For quantities in physical units we use the superscript 'phys'. The lattice action has the form

$$\sum_{\vec{n}, i} \left[ c_i^*(\vec{n}) c_i(\vec{n} + \hat{0}) - e^{\sqrt{-C\alpha_t} s(\vec{n}) + \frac{C\alpha_t}{2}} (1 - 6h) c_i^*(\vec{n}) c_i(\vec{n}) \right] - h \sum_{\vec{n}, l_s, i} \left[ c_i^*(\vec{n}) c_i(\vec{n} + \hat{l}_s) + c_i^*(\vec{n}) c_i(\vec{n} - \hat{l}_s) \right] + \frac{1}{2} \sum_{\vec{n}} (s(\vec{n}))^2. \quad (1)$$

Here  $\vec{n}$  labels the sites of a  $3 + 1$  dimensional lattice,  $\hat{l}_s$  ( $s = 1, 2, 3$ ) are the spatial lattice unit vectors,  $\hat{0}$  is a temporal lattice unit vector, and  $i$  labels the two spin components of the fermion. The temporal lattice spacing is  $a_t$ , and  $\alpha_t = a_t/a$  is the ratio of the temporal to spatial lattice spacing. We have also defined  $h = \alpha_t/(2m)$ , where  $m$  is the fermion mass in lattice units.

Our choices for the physical values of the fermion mass and lattice spacings are irrelevant to the universal physics of the unitary limit. Nevertheless it is convenient to assign some concrete values to these parameters. The values we choose are motivated by the dilute neutron system. We use a fermion mass of 939 MeV and lattice spacings  $a = (50 \text{ MeV})^{-1}$ ,

$a_t = (24 \text{ MeV})^{-1}$ . Our spatial geometry is a periodic cube of length  $L$  lattice units. The Grassmann fields are denoted by  $c_i(\vec{n})$ .  $s(\vec{n})$  is an auxiliary Hubbard-Stratonovich field which upon integration reproduces the attractive contact interaction between up and down spins. The interaction coefficient for these lattice spacings is computed by summing two-particle scattering bubble diagrams. The details of the calculation are given in [21]. Taking the scattering length  $a_{\text{scatt}} \rightarrow \infty$ , we find in the unitary limit,  $C^{\text{phys}} = -1.203 \times 10^{-4} \text{ MeV}^{-2}$ .

In order to compute the ground state energy, we consider the correlation function

$$Z_{N,N}(t) = \langle \Psi_{N,N}^0 | e^{-Ht} | \Psi_{N,N}^0 \rangle, \quad (2)$$

where the initial/final state  $|\Psi_{N,N}^0\rangle$  is the normalized Slater determinant ground state for the free  $N, N$  particle system. We refer to  $t$  as the Euclidean time. We define

$$E_{N,N}(t) = -\frac{\partial}{\partial t} [\ln Z_{N,N}(t)]. \quad (3)$$

Then as  $t \rightarrow +\infty$ ,  $E_{N,N}(t)$  converges to  $E_{N,N}^0$ , the ground state energy of the interacting  $N, N$  particle system. The only assumption is that the ground state has a nonvanishing overlap with the ground state of the non-interacting system.

For the non-interacting system we find  $E_{N,N}^{\text{free}}(t) = E_{N,N}^{0,\text{free}}$ , where  $E_{N,N}^{0,\text{free}}$  is the free Fermi ground state energy. It is useful to define the dimensionless function

$$\xi_{N,N}(t) = \frac{E_{N,N}(t)}{E_{N,N}^{0,\text{free}}}. \quad (4)$$

In the unitary limit  $\xi_{N,N}(t)$  depends only on the dimensionless combination  $\frac{t}{mL^2}$ . We can define the Fermi energy,

$$E_F = \frac{k_F^2}{2m} = \frac{1}{2m} (3\pi^2 \rho)^{2/3} \simeq 7.596 \frac{N^{2/3}}{mL^2}, \quad (5)$$

where  $k_F$  is the Fermi momentum. In the unitary limit we can regard  $\xi_{N,N}(t)$  as a function of  $E_F t$ , and for sufficiently large  $N$  it should approach a common asymptotic form.

The conversion of the Grassmann lattice action to a worldline formalism at fixed particle number has been detailed in [22]. We use the same transfer matrix derived there, except in this case we keep the auxiliary Hubbard-Stratonovich field and calculate the integral over auxiliary field configurations,

$$Z_{N,N}(t) \propto \int Ds e^{-\frac{1}{2} \sum_{\vec{n}} (s(\vec{n}))^2} \langle \Psi_{N,N}^0 | T e^{-H(s)t} | \Psi_{N,N}^0 \rangle. \quad (6)$$

The advantage of the auxiliary field formalism is that  $H(s)$  consists of only single-body operators interacting with the background auxiliary field. We can therefore compute the full  $N, N$ -body matrix element as the square of the determinant of the single-particle matrix elements,

$$\langle \Psi_{N,N}^0 | T e^{-H(s)t} | \Psi_{N,N}^0 \rangle \propto [\det M(s, t)]^2, \quad (7)$$

$$M_{ij}(s, t) = \langle p_i | T e^{-H(s)t} | p_j \rangle, \quad (8)$$

where  $i, j$  go from 1 to  $N$ . The states  $|p_j\rangle$  are single-particle momentum states comprising our Slater determinant initial/final state. The square of the determinant arises from the fact that the single-body operators in  $H(s)$  are the same for both up and down spins. Since the square of the determinant is nonnegative, there is no sign problem in this formalism.

Our notation,  $T e^{-H(s)t}$ , is shorthand for the time-ordered product of single-body transfer matrices at each time step,

$$T e^{-H(s)t} = M(L_t - 1) \cdot \dots \cdot M(n_t) \cdot \dots \cdot M(1) \cdot M(0), \quad (9)$$

where  $L_t$  is the total number of lattice time steps and  $t = L_t a_t$ . If the particle stays at the same spatial lattice site from time step  $n_t$  to  $n_t + 1$ , then the corresponding matrix element of  $M(n_t)$  is

$$e^{\sqrt{-C\alpha_t} s(\vec{n}) + \frac{C\alpha_t}{2}} (1 - 6h). \quad (10)$$

If the particle hops to a neighboring lattice site from time step  $n_t$  to  $n_t + 1$  then the corresponding matrix element of  $M(n_t)$  is  $h$ . All other elements of  $M(n_t)$  are zero.

### III. ENDPOINT IMPORTANCE SAMPLING AND HYBRID MONTE CARLO

While there is no sign problem, the calculation of  $Z_{N,N}(t)$  is not straightforward. Due to the large coupling strength in the unitary limit, fluctuations in  $[\det M(s, t)]^2$  are very large. We deal with this problem by sampling configurations according to the weight

$$\exp \left\{ -\frac{1}{2} \sum_{\vec{n}} (s(\vec{n}))^2 + 2 \log [|\det M(s, t_{\text{end}})|] \right\}, \quad (11)$$

where  $t_{\text{end}}$  is the largest Euclidean time at which we wish to measure  $Z_{N,N}(t)$ . It is most efficient to sample configurations using a non-local updating method called hybrid Monte

Carlo [23]. A description of the hybrid Monte Carlo method as applied to the grand canonical ensemble of spin-1/2 neutrons can be found in [21]. For this fixed particle number simulation we compute molecular dynamics trajectories for

$$H(s, p) = \frac{1}{2} \sum_{\vec{n}} (p(\vec{n}))^2 + V(s), \quad (12)$$

where  $p(\vec{n})$  is the conjugate momentum for  $s(\vec{n})$  and

$$V(s) = \frac{1}{2} \sum_{\vec{n}} (s(\vec{n}))^2 - 2 \log [|\det M(s, t_{\text{end}})|]. \quad (13)$$

The steps of the algorithm are as follows.

Step 1: Select an arbitrary initial configuration  $s^0(\vec{n})$ .

Step 2: Select  $p^0(\vec{n})$  according to the Gaussian random distribution

$$P(p^0(\vec{n})) \propto \exp \left[ -\frac{1}{2} (p^0(\vec{n}))^2 \right]. \quad (14)$$

Step 3: Let

$$\tilde{p}^0(\vec{n}) = p^0(\vec{n}) - \frac{\varepsilon}{2} \left[ \frac{\partial V(s)}{\partial s(\vec{n})} \right]_{s=s^0} \quad (15)$$

for some small positive  $\varepsilon$ . In computing the derivative of  $V$ , we use the fact that

$$\begin{aligned} \frac{\partial V(s)}{\partial s(\vec{n})} &= s(\vec{n}) - \frac{2}{\det M} \sum_{k,l} \frac{\partial \det M}{\partial M_{kl}} \frac{\partial M_{kl}}{\partial s(\vec{n})} \\ &= s(\vec{n}) - 2 \sum_{k,l} [M^{-1}]_{lk} \frac{\partial M_{kl}}{\partial s(\vec{n})}. \end{aligned} \quad (16)$$

Step 4: For  $j = 0, 1, \dots, N-1$ , let

$$s^{j+1}(\vec{n}) = s^j(\vec{n}) + \varepsilon \tilde{p}^j(\vec{n}), \quad (17)$$

$$\tilde{p}^{j+1}(\vec{n}) = \tilde{p}^j(\vec{n}) - \varepsilon \left[ \frac{\partial V(s)}{\partial s(\vec{n})} \right]_{s=s^{j+1}}. \quad (18)$$

Step 5: Let

$$p^N(\vec{n}) = \tilde{p}^N(\vec{n}) + \frac{\varepsilon}{2} \left[ \frac{\partial V(s)}{\partial s(\vec{n})} \right]_{s=s^N}. \quad (19)$$

Step 6: Select a random number  $r \in [0, 1)$ . If

$$r < \exp [-H(s^N, p^N) + H(s^0, p^0)] \quad (20)$$

then let

$$s^0(\vec{n}) = s^N(\vec{n}). \quad (21)$$

Otherwise leave  $s^0$  as is. In either case go back to Step 2.

For each configuration the observables that we calculate are

$$O(s, t) = \frac{[\det M(s, t)]^2}{[\det M(s, t_{\text{end}})]^2}, \quad (22)$$

for  $t < t_{\text{end}}$ . By taking the ensemble average of  $O(s, t)$  we are able to calculate

$$\frac{Z_{N,N}(t)}{Z_{N,N}(t_{\text{end}})}. \quad (23)$$

Fluctuations in the observable  $O(s, t)$  are manageable in size so long as  $t_{\text{end}} - t$ , the temporal separation from the endpoint, is not too large. This is typically not a problem since only a small window in  $t$  near  $t_{\text{end}}$  is needed to calculate  $-\frac{\partial}{\partial t} [\ln Z_{N,N}(t)]$  at  $t = t_{\text{end}}$ . For each simulation we compute roughly  $2 \times 10^5$  hybrid Monte Carlo trajectories, split across four processors running completely independent trajectories. Averages and errors are computed by comparing the results of each processor.

#### IV. ERROR ESTIMATES

We use double precision arithmetic to compute  $\det M(s, t_{\text{end}})$  and  $O(s, t)$ . We carefully monitor any systematic errors produced by double precision round off error and exceptional configurations. To do this we introduce a small positive parameter  $\epsilon$  and reject any hybrid Monte Carlo trajectories which generate a configuration with

$$|\det M| < \epsilon^N \prod_{i=1, \dots, N} |M_{ii}|. \quad (24)$$

We then take the limit  $\epsilon \rightarrow 0^+$  to determine if poorly condition matrices make any detectable contribution to our observable. We consider values for  $\epsilon$  as small as  $10^{-6}$ . If as we take  $\epsilon \rightarrow 0^+$  any systematic error can be detected above the stochastic error level, then we throw out the measurement and do not include it in the final results. The error bars we present

are therefore estimates of the total error for each lattice system. There are no additional errors other than the lattice spacing dependence.

Errors due to finite lattice spacing can be estimated by the spread of  $\xi_{N,N}(t)$  at fixed  $N$  for different lattice lengths  $L$ . By fitting the data for different  $L$  to a single function  $\xi_{N,N}(t)$ , we can compute the uncertainty in the fit parameters and estimate the error of the measurement in the continuum limit. Therefore the error bars on our final results include both systematic and stochastic errors for each lattice system as well as systematic errors due to lattice spacing dependence.

## V. RESULTS

As a first test we consider the 1,1 particle system. In this case the free Fermi ground state energy  $E_{1,1}^{0,\text{free}}$  is zero. So instead of dividing by  $E_{1,1}^{0,\text{free}}$ , we measure the dimensionless quantity  $mL^2 E_{1,1}(t)$ . In Table 1  $mL^2 E_{1,1}(t)$  is shown for various  $t$  and  $L$ . We also show the results for the dimensionless interacting ground state energy,  $mL^2 E_{1,1}^0$ , as computed by summing lattice bubble diagrams.

Table 1:  $mL^2 E_{1,1}(t)$  for various  $t$  and  $L$

$L$	$12a_t$	$24a_t$	$36a_t$	$48a_t$	$60a_t$	$mL^2 E_{1,1}^0$
4	-2.7(1)	-3.4(1)	-3.4(1)	-3.4(1)	-3.5(1)	-3.57
5	-2.5(1)	-3.1(1)	-3.5(1)	-3.5(1)	-3.5(1)	-3.60
6	-2.0(1)	-2.7(1)	-3.1(1)	-3.6(1)	-3.5(1)	-3.62

For large  $t$  we see that  $mL^2 E_{1,1}(t)$  matches  $mL^2 E_{1,1}^0$  within error bars. For large  $L$  the lattice discretization error should be negligible and  $mL^2 E_{1,1}^0$  should approach the unitary limit result,

$$4\pi^2 d_1 \simeq 4\pi^2(-0.095901) \simeq -3.7860, \quad (25)$$

where  $d_1$  is the large scattering length expansion coefficient in a periodic cube as defined in [24]. We see that  $mL^2 E_{1,1}^0$  is within a few percent of the unitary limit value for  $L = 4, 5, 6$ .

We have performed hybrid Monte Carlo simulations of the  $N = 3, 5, 7, 9$  systems with lattice lengths  $L = 4, 5, 6$  and the  $N = 11$  system with lattice lengths  $L = 5, 6$ . In Figs. 1, 2, 3, 4, 5 we show  $\xi_{N,N}(t)$  as a function of  $E_F t$  for  $N = 3, 5, 7, 9, 11$  respectively.

In all cases we find agreement in  $\xi_{N,N}(t)$  for different values of  $L$ , indicating the physics



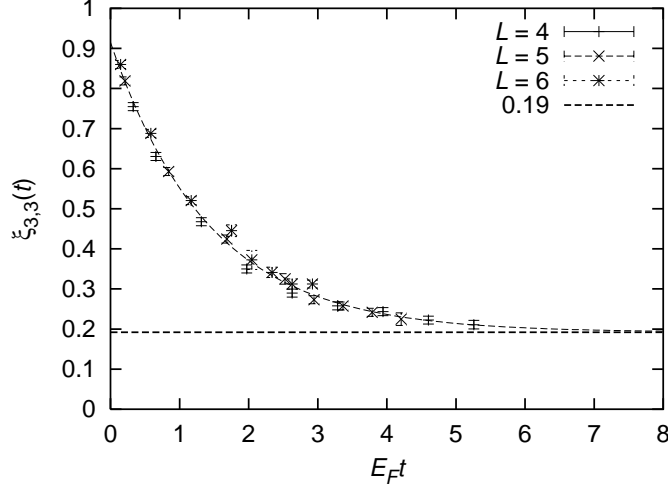


FIG. 1:  $\xi_{3,3}(t)$  versus  $E_F t$  for  $L = 4, 5, 6$ .

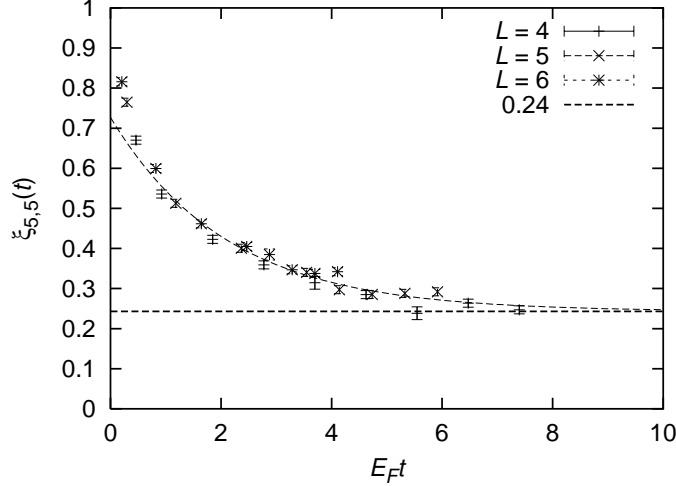


FIG. 2:  $\xi_{5,5}(t)$  versus  $E_F t$  for  $L = 4, 5, 6$ .

signature of the unitary limit. The agreement for different values of  $L$  shows that to a good approximation  $L$  is the only dimensionful scale in the system. The lack of any significant corrections due to varying  $L$  indicates that the lattice discretization error is small and that the scattering length is essentially infinite. This provides a non-trivial check within the context of the many body system that the physics is consistent with the unitary limit. We find that detuning the coupling constant away from the unitary limit value by as little as 5% in either direction produces a measurable disagreement in  $\xi_{N,N}(t)$  for different values of

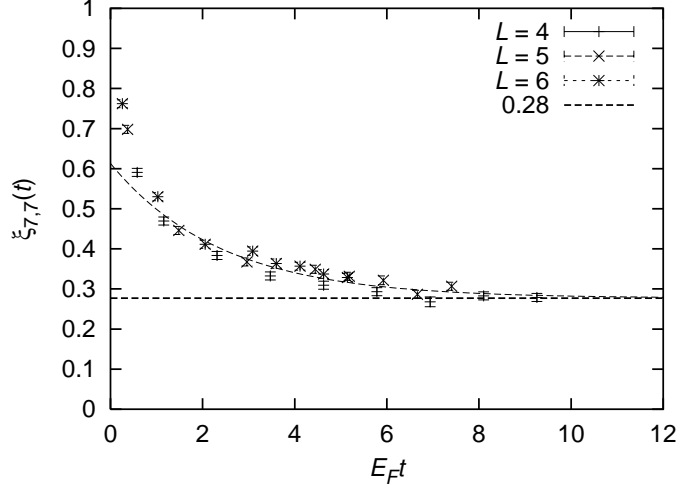


FIG. 3:  $\xi_{7,7}(t)$  versus  $E_F t$  for  $L = 4, 5, 6$ .

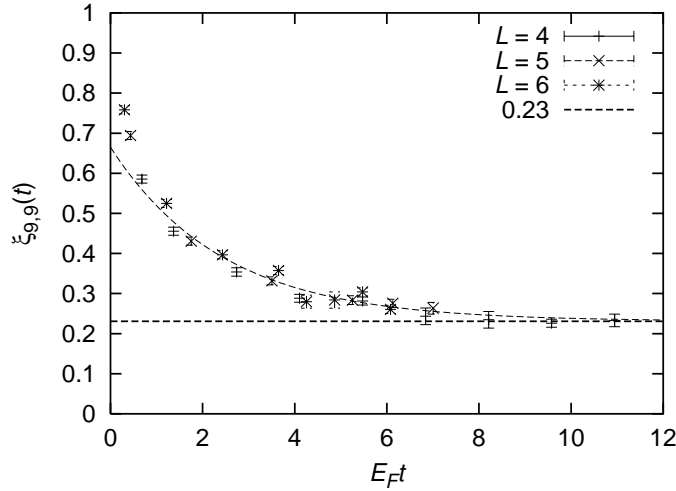


FIG. 4:  $\xi_{9,9}(t)$  versus  $E_F t$  for  $L = 4, 5, 6$ .

$L$ . We discuss this further in the next section.

We fit  $\xi_{N,N}(t)$  at large  $E_F t$  to the functional form  $b + c \exp(-\delta \cdot E_F t)$  to determine the asymptotic value as  $E_F t \rightarrow \infty$ . This is the asymptotic form one expects for very large  $E_F t$ , where  $\delta \cdot E_F$  is the gap in the energy spectrum above the ground state energy  $E_{N,N}^0$ . If there is a non-negligible coupling to gapless phonon modes, then  $\delta$  should go to zero as we increase the number of particles and volume. However it is not clear which excited states have a non-negligible overlap with our free particle initial/final state. It is also unclear if

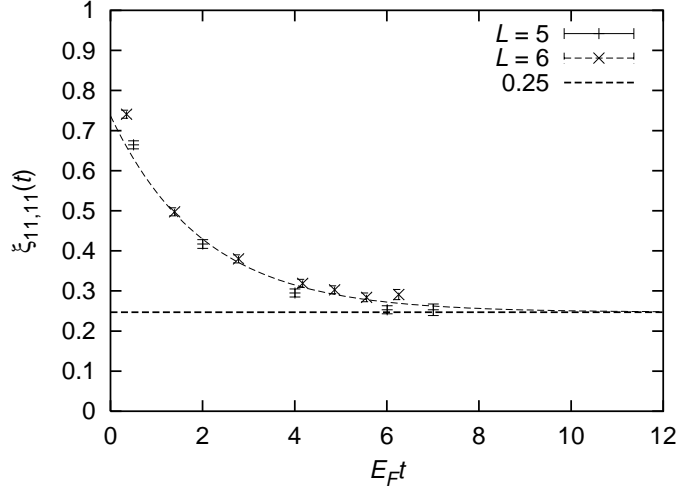


FIG. 5:  $\xi_{11,11}(t)$  versus  $E_F t$  for  $L = 5, 6$ .

we are probing at sufficiently large  $E_F t$  and with sufficient accuracy to determine  $\delta$  reliably. We hope to resolve these questions with future studies. For our purposes here we consider  $\delta$  only as a fit parameter to determine the asymptotic value for  $\xi_{N,N}(t)$  at large  $E_F t$ .

The ratio of the ground state energy of the interacting system to the free particle ground state energy is given by the large  $E_F t$  limit of  $\xi_{N,N}(t)$ . The results for these ratios are shown in Table 2.

Table 2: Results for  $E_{N,N}^0/E_{N,N}^{0,\text{free}}$

$N = 3$	$N = 5$	$N = 7$	$N = 9$	$N = 11$
0.19(2)	0.24(2)	0.28(2)	0.23(2)	0.25(2)

From Table 2 we see that the energy ratio for the smallest system,  $N = 3$ , is somewhat lower than the rest. However the ratios for  $N \geq 5$  are close to a central value of about 0.25. Assuming no large changes to this ratio for  $N > 11$ , we estimate that  $\xi = 0.25(3)$ .

In Fig. 6 we show simultaneously all of the plots of  $\xi_{N,N}(t)$  as a function of  $E_F t$ . We see again that the smallest system,  $N = 3$ , is somewhat different from the rest, falling off with a faster exponential at large  $E_F t$ . The curves for  $N = 5, 7, 9, 11$  seem quite similar in both shape and asymptotic value, suggesting that the curves are already close to the large  $N$  limit.

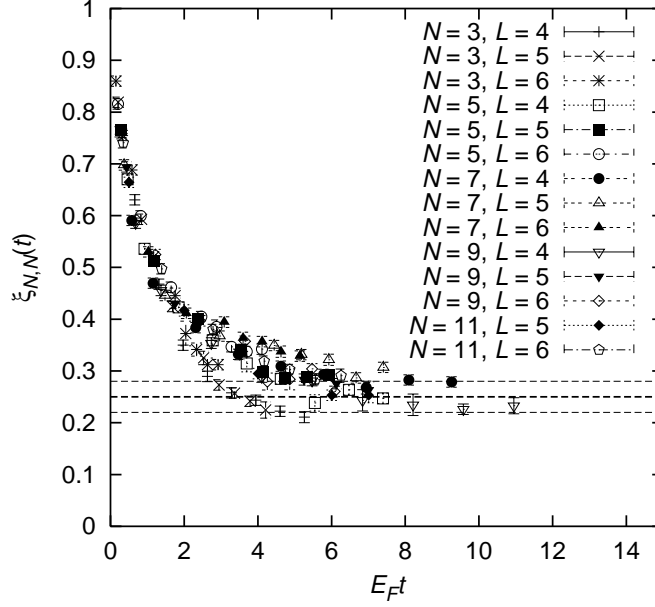


FIG. 6:  $\xi_{N,N}(t)$  versus  $E_F t$  for  $N = 3, 5, 7, 9, 11$ . We have drawn lines showing the central value and error bounds for the estimate  $\xi = 0.25(3)$ .

## VI. DISCUSSION AND ADDITIONAL CROSS-CHECKS

Our result  $\xi = 0.25(3)$  disagrees with the fixed-node Green's function Monte Carlo results  $\xi = 0.44(1)$  [14] and  $0.42(1)$  [15]. However it is consistent with the requirement that the fixed-node value sets a variational upper bound on the energy. One explanation of the disagreement could be the difficulty in determining a lower bound for  $\xi$  using Green's function Monte Carlo. This requires removing the nodal constraint and overcoming a sign problem that scales exponentially with  $N$ . But in any case the disagreement of our final result and published fixed-node results suggests further tests of the robustness of our method. We consider three additional cross-checks in this section.

The first test we consider is whether or not the non-quadratic lattice dispersion relation is significantly affecting our results. While deviations were found in nonzero temperature simulations [19], the fact that  $\xi_{N,N}(t)$  is the same for different values of  $L$  suggests that this is not the case at zero temperature. However if we are measuring true continuum limit behavior, it should be possible to reproduce the same results using a different lattice action with the same continuum limit. To carry out this cross-check we consider an  $O(a^2)$ -improved action with next-to-nearest neighbor hopping that reproduces the continuum dispersion

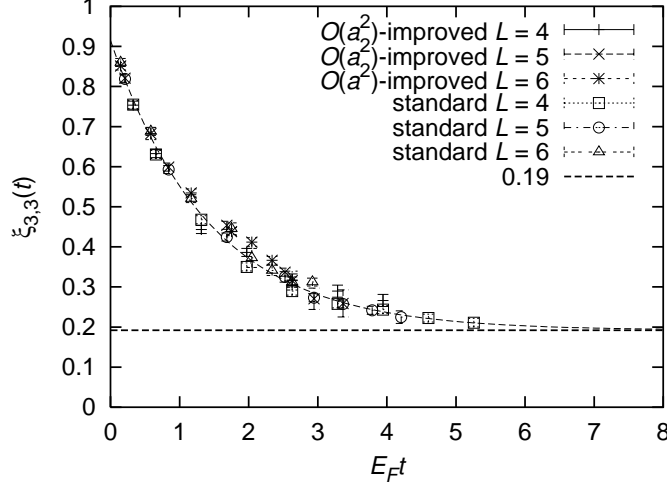


FIG. 7:  $O(a^2)$ -improved and standard lattice action results for  $\xi_{3,3}(t)$  versus  $E_F t$  for  $L = 4, 5, 6$ .

relation  $p^2/(2m)$  up to  $O(p^6)$ . Instead of the standard action (1), we use the improved action

$$\begin{aligned}
& \sum_{\vec{n}, i} \left[ c_i^*(\vec{n}) c_i(\vec{n} + \hat{0}) - e^{\sqrt{-C\alpha_t} s(\vec{n}) + \frac{C\alpha_t}{2}} \left(1 - \frac{15}{2} h\right) c_i^*(\vec{n}) c_i(\vec{n}) \right] \\
& - \frac{4}{3} h \sum_{\vec{n}, l_s, i} \left[ c_i^*(\vec{n}) c_i(\vec{n} + \hat{l}_s) + c_i^*(\vec{n}) c_i(\vec{n} - \hat{l}_s) \right] \\
& + \frac{1}{12} h \sum_{\vec{n}, l_s, i} \left[ c_i^*(\vec{n}) c_i(\vec{n} + 2\hat{l}_s) + c_i^*(\vec{n}) c_i(\vec{n} - 2\hat{l}_s) \right] + \frac{1}{2} \sum_{\vec{n}} (s(\vec{n}))^2. \quad (26)
\end{aligned}$$

As before we calculate the interaction coefficient by summing two-particle scattering bubble diagrams. We find in the unitary limit,  $C^{\text{phys}} = -1.581 \times 10^{-4} \text{ MeV}^{-2}$ .

The results for  $N = 3$  are shown in Fig. 7. We have taken the standard lattice action results shown in Fig. 1 and superimposed the new  $O(a^2)$ -improved lattice data. There is almost no difference between the standard and  $O(a^2)$ -improved lattice results. This suggests that we are measuring continuum limit behavior.

The second test we consider is whether the interaction coefficient can be retuned to recover the fixed-node value for  $\xi$  while approximately retaining the physics of the unitary limit. In order to test this possibility we consider the  $N = 5$  system. We tune the interaction coefficient so that for  $L = 4$  we get  $\lim_{t \rightarrow \infty} \xi_{5,5}(t) = 0.42$ . By trial and error we find that this occurs for  $C^{\text{phys}} = -1.08 \times 10^{-4} \text{ MeV}^{-2}$ , which is about 90% of the unitary limit value. In the two-particle system this corresponds with a scattering length of  $a_{\text{scatt}} \simeq -7.0 \text{ fm}$

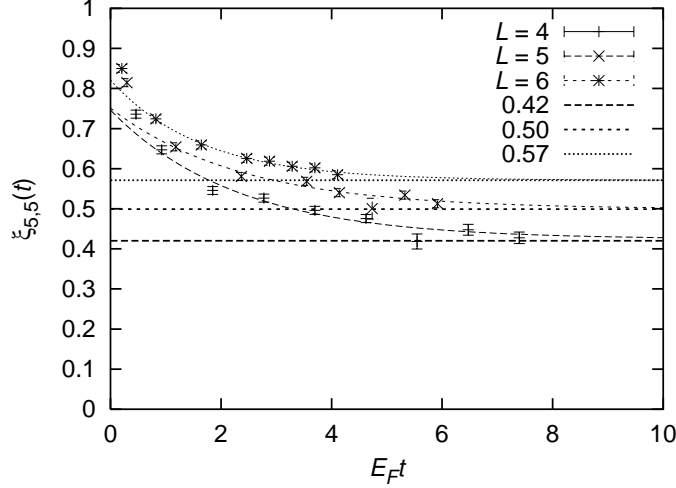


FIG. 8:  $\xi_{5,5}(t)$  versus  $E_F t$  for  $L = 4, 5, 6$  and  $C^{\text{phys}} = -1.08 \times 10^{-4} \text{ MeV}^{-2}$ .

$\simeq -0.035 \text{ MeV}^{-1}$ .

We now simulate the system for  $L = 5$  and  $L = 6$ . The results are shown in Fig. 8. The plots for  $\xi_{5,5}(t)$  do not agree for different  $L$ , and we find  $\lim_{t \rightarrow \infty} \xi_{5,5}(t) = 0.42, 0.50, 0.57$  for  $L = 4, 5, 6$  respectively. From these results it appears that  $\lim_{t \rightarrow \infty} \xi_{5,5}(t) = 0.42$  is inconsistent with the unitary limit. In fact we can use this data to estimate the finite scattering length correction. Using  $a_{\text{scatt}} \simeq -0.035 \text{ MeV}^{-1}$  we find

$$\lim_{t \rightarrow \infty} \xi_{5,5}(t) \approx 0.24 - 0.6 \cdot k_F^{-1} a_{\text{scatt}}^{-1}. \quad (27)$$

A more thorough study of the finite scattering length correction to  $\xi$  will be presented in future work.

The third test we consider is whether the same ground state energy can be extracted using different initial/final states. We test this using the  $N = 7$  system with  $L = 4$ . We define  $|\Psi_{7,7}^2\rangle$  as the state we get by taking  $|\Psi_{7,7}^0\rangle$  and removing the four fermions at momentum  $(p_x, p_y, p_z) = (0, 0, \pm \frac{2\pi}{aL})$  and setting them at higher momentum,  $(p_x, p_y, p_z) = (\pm \frac{2\pi}{aL}, \pm \frac{2\pi}{aL}, 0)$ . We define  $|\Psi_{7,7}^1\rangle$  in the same way, except we put only two fermions at the higher momentum while keeping the total momentum equal to zero.

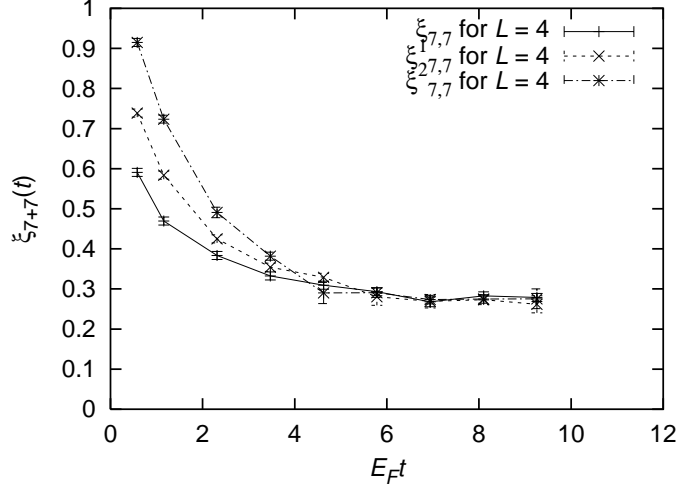


FIG. 9: Comparison of  $\xi_{7,7}(t)$ ,  $\xi_{7,7}^1(t)$ , and  $\xi_{7,7}^2(t)$ .

We define the following quantities using the excited Slater determinant states:

$$Z_{7,7}^1(t) = \langle \Psi_{7,7}^1 | e^{-Ht} | \Psi_{7,7}^1 \rangle, \quad Z_{7,7}^2(t) = \langle \Psi_{7,7}^2 | e^{-Ht} | \Psi_{7,7}^2 \rangle, \quad (28)$$

$$E_{7,7}^1(t) = -\frac{\partial}{\partial t} [\ln Z_{7,7}^1(t)], \quad E_{7,7}^2(t) = -\frac{\partial}{\partial t} [\ln Z_{7,7}^2(t)], \quad (29)$$

$$\xi_{7,7}^1(t) = \frac{E_{7,7}^1(t)}{E_{7,7}^{0,\text{free}}}, \quad \xi_{7,7}^2(t) = \frac{E_{7,7}^2(t)}{E_{7,7}^{0,\text{free}}}. \quad (30)$$

The comparison of  $\xi_{7,7}(t)$ ,  $\xi_{7,7}^1(t)$ , and  $\xi_{7,7}^2(t)$  is shown in Fig. 9. The convergence of all three results at large  $E_F t$  suggests that we are measuring the true ground state energy at large  $E_F t$ .

## VII. SUMMARY

We have measured the ground state energy for  $N, N$  spin-1/2 fermions in the unitary limit in a periodic cube. Our results at  $N = 3, 5, 7, 9, 11$  suggest that for large  $N$  the ratio of the ground state energy to that of a free Fermi gas is  $0.25(3)$ . Our result lies in the middle of the bound  $0.07 \leq \xi \leq 0.42$  given in [20]. Although it is inconsistent with the fixed-node Green's function Monte Carlo results  $\xi = 0.44(1)$  [14] and  $0.42(1)$  [15], it is consistent with the requirement that the fixed-node value sets a variational upper bound on the energy. We have cross-checked the robustness of our results by comparing with an  $O(a^2)$ -improved action, detuning away from the unitary limit to measure deviations, and

using different initial/final states to reproduce the same ground state energy. In this paper we have not addressed the questions of the existence of superfluidity, long range order, or the pairing gap. However the methods presented here shows some promise at probing some of these interesting questions.

Acknowledgments: The author is grateful to Thomas Schäfer for many helpful discussions. This work is supported by the US Department of Energy grant DE-FG02-04ER41335.

- 
- [1] K. M. O'Hara, S. L. Hemmer, M. E. Gehm, S. R. Granade, and J. E. Thomas, *Science* **298**, 2179 (2002).
  - [2] S. Gupta, Z. Hadzibabic, M. W. Zwierlein, C. A. Stan, K. Dieckmann, C. H. Schunck, E. G. M. van Kempen, B. J. Verhaar, and W. Ketterle, *Science* **300**, 1723 (2003).
  - [3] C. A. Regal and D. S. Jin, *Phys. Rev. Lett.* **90**, 230404 (2003).
  - [4] T. Bourdel, J. Cubizolles, L. Khaykovich, K. M. F. Magalhaes, S. J. J. M. F. Kokkelmans, G. V. Shlyapnikov, and C. Salomon, *Phys. Rev. Lett.* **91**, 020402 (2003).
  - [5] M. E. Gehm, S. L. Hemmer, S. R. Granade, K. M. O'Hara, and J. E. Thomas, *Phys. Rev.* **A68**, 011401(R) (2003).
  - [6] J. Kinast, A. Turlapov, J. E. Thomas, Q. Chen, J. Stajic, and K. Levin, *Science* **307**, 1296 (2005), cond-mat/0502087.
  - [7] M. Bartenstein, A. Altmeyer, S. Riedl, S. Jochim, C. Chin, J. Hecker Denschlag, and R. Grimm, *Phys. Rev. Lett.* **92**, 120401 (2004).
  - [8] C. J. Pethick and D. G. Ravenhall, *Ann. Rev. Nucl. Part. Sci.* **45**, 429 (1995).
  - [9] J. R. Engelbrecht, M. Randeria, and C. S. de Melo, *Phys. Rev.* **B55**, 15153 (1997).
  - [10] H. Heiselberg, *Phys. Rev. A* **63**, 043606 (2001), cond-mat/0002056.
  - [11] T. Schafer, C.-W. Kao, and S. R. Cotanch, *Nucl. Phys.* **A762**, 82 (2005), nucl-th/0504088.
  - [12] A. Perali, P. Pieri, and G. C. Strinati, *Phys. Rev. Lett.* **93**, 100404 (2004).
  - [13] G. A. Baker, *Phys. Rev.* **C60**, 054311 (1999).
  - [14] J. Carlson, S. Y. Chang, V. R. Pandharipande, and K. Schmidt, *Phys. Rev. Lett.* **91**, 50401 (2003), physics/0303094.
  - [15] G. E. Astrakharchik, J. Boronat, J. Casulleras, and S. Giorgini, *Phys. Rev. Lett.* **93**, 200404 (2004), cond-mat/0406113.



- [16] T. Papenbrock, Phys. Rev. A **72**, 041603 (2005), cond-mat/0507183.
- [17] M. Wingate (2005), cond-mat/0502372.
- [18] A. Bulgac, J. E. Drut, and P. Magierski (2005), cond-mat/0505374.
- [19] D. Lee and T. Schafer (2005), nucl-th/0509017.
- [20] D. Lee and T. Schafer (2005), nucl-th/0509018.
- [21] D. Lee and T. Schaefer, Phys. Rev. **C72**, 024006 (2005), nucl-th/0412002.
- [22] B. Borasoy, H. Krebs, D. Lee, and U. G. Meissner (2005), nucl-th/0510047.
- [23] S. Duane, A. D. Kennedy, B. J. Pendleton, and D. Roweth, Phys. Lett. **B195**, 216 (1987).
- [24] S. R. Beane, P. F. Bedaque, A. Parreno, and M. J. Savage, Phys. Lett. **B585**, 106 (2004), hep-lat/0312004.